

Acoustic emission and damage evolution at mean temperature under air of a SiC/[Si-B-C] composite subjected to cyclic and static loading : towards lifetime prediction

E. Racie, N. Godin, P. Reynard, M. R'Milli and G. Fantozzi
INSA de Lyon, laboratoire MATEIS, 7 avenue Jean Capelle, 69621 Villeurbanne cedex

ABSTRACT: The low density and the high tensile strength of Ceramic Matrix Composites (CMC) make them a good technical solution to design aeronautical structural components. To fully understand damage mechanisms and be able to design components, its behavior has to be analyzed during fatigue tests. The aim of the present study is to consider the possibility of predicting rupture time from acoustic emission monitoring. New indicators of damage are defined, based on acoustic energy. These indicators highlight critical times or characteristic times allowing an evaluation of the remaining lifetime.

1 INTRODUCTION

Ceramic matrix composites (CMC) seem to be adequate materials to design new generation of civil aircraft engines because of their low density and high tensile strength at high temperature. That is why damage mechanisms have to be identified, through cyclic fatigue tests.

The aim of the study consists in analyzing and comparing material behavior under cyclic and static fatigue loadings, at the same temperature and under air, to determine the effects of a cyclic loading on damage and lifetime. CMCs seem to be promising material for aeronautical applications, even if their constituent materials are brittle, the strain at failure is rather high due to considerable matrix cracking and cracks deflection at interfaces [1]. However, the behavior of these materials is affected by oxidation of interphases, fibers and the ultimate failure is governed by slow crack growth in fibers [2]. Self-healing material has been developed to protect fibers against oxidation, which increased largely the lifetime of material. Nevertheless, under air and for temperature under 550°C, self-healing is not significant enough to fully protect the material. It's therefore important to understand the material behavior for those temperatures. As specified above, the lifetimes under these types of loadings are rather long, which makes it hard to realize tests on laboratory equipment. This kind of studies needs to be done with a limited number of tests, thus the use of different techniques to monitor the damage in real time is mandatory. Acoustic emission (AE) appears to be a good candidate in this case. The aim of AE is to record transient elastic waves on the material created by damage mechanisms. There are several studies referring to this kind of method for different types of CMCs under tensile tests [3-5]. For fatigue tests, damage can be analyzed from different points of view, first by linking each acoustical event to the damage mechanism which generated it [5-6]. This process needs clustering algorithms [7]. Another approach consists in considering the evolution of released energy [8-10]. It is generally accepted that the energy of an AE signal is related to the energy released by the source. Consequently, AE energy gives information about material damage; it is then possible to point out precursory elements to ultimate failure or to simulate AE energy evolution with a power law to determine lifetime.

A main purpose of this paper is to consider the possibility of predicting rupture time of CMC from damage evolution recorded by AE technique. The objective of this approach is to propose a method based on acoustic energy in order to evaluate the remaining lifetime during long-term-mechanical tests. The approach is based on the determination of energy released and identification of a critical point in energy release during mechanical test. So beyond this characteristic point, the criticality can be modeled with a power-law in order to evaluate time to failure.

In this study, new indicators of damage have been defined, based mainly on acoustic energy analysis. These indicators highlight critical times or characteristic times allowing an evaluation of the remaining lifetime. Moreover, the clustering of acoustic emission, using a supervised clustering method based on random forest approach [11], makes possible to get a real-time detection of each damage phenomena and to identify the mechanism responsible for this critical time.

2 EXPERIMENTAL PROCEDURE

2.1 *Materials and mechanical tests*

Fatigue tests have been realised at a temperature of 450°C under air. The material is a ceramic matrix composite reinforced with Nicalon SiC fibers, coated with PyC and embedded in a self-healing [Si-B-C] matrix. The reinforcement architecture is a stack of several layers of 2D satin fabrics linked together by strands of fibers in the third direction. In this study all the specimens have a dog-bone shape with a thickness of 4 mm and a gauge section



of 60 mm x 16 mm. For static fatigue tests, specimens were first loaded at constant loading rate of 1kN/min, and periodically (every 6 or 12 hours) unloading-reloading cycles were carried out in order to determine the secant elastic modulus. Cyclic fatigue tests were conducted under a tensile/tensile sinusoidal loading with constant amplitude and a frequency of 2 Hz. Strain is measured using an extensometer. In the case of static fatigue tests, the imposed stress increases every T_i (time for 18% of N_f , number of cycles to failure) with a step corresponding to 6 % of tensile strength. At the same time cyclic fatigue tests are realized with imposed stress oscillating at a frequency of 2 Hz between 0 and a constant maximum value which is incremented of 6 % every 18% of N_f (Fig. 1). Moreover, cyclic fatigue tests with constant amplitude were conducted under a tensile/tensile sinusoidal loading and a frequency of 2 Hz until composite fracture.

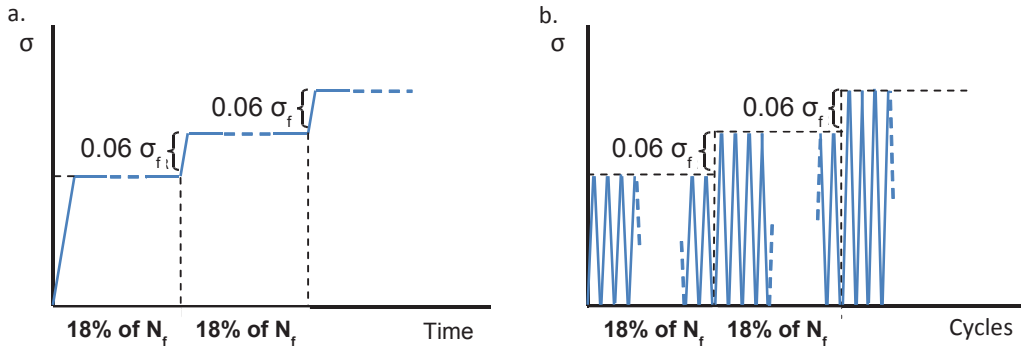


Figure 1. Applied stress for a. Incremental static fatigue test b. Incremental cyclic fatigue test

2.2 Acoustic emission monitoring

Two piezoelectric sensors (Micro80, Mistras Group) are maintained on the specimen surface. Medium viscosity vacuum grease is used to ensure a good coupling between the specimen and sensors. Each sensor is connected to the data acquisition system (PCI2, Mistras Group) via a preamplifier with a 40 dB gain and 20-1200 kHz bandwidth (Mistras Group).

During tests, AE is recorded with 2 piezoelectric sensors, one on each side of the reduced section. The position of a detected source can be determined linearly knowing the wave velocity in the material.

The AE wave velocity has been calibrated before the test Ce_0 , according to a pencil lead break procedure: several breaks were performed on the specimen at several locations x between the two sensors. The velocity $C_e(\varepsilon)$ of an extensional wave in a thin plate is proportional to the square root of the elastic modulus E of the material. Since E decreases as damage occurs in the material, it is important to take into account the evolution of C_e during the mechanical test in order to better evaluate the location of the AE sources. As proposed by Morsher [4], the initial modulus during unloading $E(\varepsilon)$ was measured during a cycled tensile test, where hysteresis loops were obtained at different strains. The velocity $C_e(\varepsilon)$ was then determined by using equation 1:

$$\frac{C_e(\varepsilon)}{C_{e_0}} = \sqrt{\frac{E(\varepsilon)}{E_0}} \quad (1)$$

2.3 Damage indicators

The energy of the recorded AE events represents a part of the elastic energy released by damages of CMC specimens. Thus, the evolution of elastic energy released by analysing the energy of AE events may be investigated. The source energy $E(n)$ is then defined as the square root of the product of the amounts of energy received at both sensors $E_i(n)$ for each source:

$$E(n) = \sqrt{E_1(n) \times E_2(n)} \quad (2)$$

The first indicator is based on the coupling of mechanical energy (U_m) and acoustic energy (U_{AE}) denoted Sentry Function (F), initially introduced by Minak [12, 13]:

$$F = \ln \frac{U_m}{U_{AE}} \quad (3)$$

where U_m is strain energy and U_{AE} the cumulated acoustical energy ($\sum E_n$). F can be function of time or strain. It is defined as soon as the first acoustical event is recorded. Strain energy is calculated measuring the area under the force-displacement curve. To determine only the effects of tension, unloading/loading loads are not taken into consideration. The function is calculated every k acoustic sources ($k \sim 0.1\%$ of number of signals).

The coefficient of emission R_{AE} is defined as the increment of energy ΔE recorded during an increment of time Δt , divided by the total energy emitted during the initial loading of the sample:

$$R_{AE}(t) = \frac{1}{E_{loading}} \frac{\Delta E}{\Delta t} \quad (4)$$

where $E_{loading}$ is the cumulative AE energy for all the signals recorded during the initial loading up to the nominal load of the test, ΔE is the cumulative AE energy for all signals recorded during the interval $[t; t + \Delta t]$.

In this study the energy rather than the signal strength is used to define the severity. It is defined as the average energy.

$$S_r = \frac{1}{J} \sum_{m=1}^{m=J} E_m(n) \quad (5)$$

J is an empirical constant.

The indicator denoted R_{LU} , is defined by the ratio of the liberated energy during the loading part of a cycle and the energy recorded during the unloading part of this cycle.

$$R_{LU} = \frac{\Delta E_{loading}}{\Delta E_{unloading}} \quad (6)$$

3 RESULTS AND DISCUSSION

Results of fatigue tests are summarized in Table 1. To compare the results of static and cyclic fatigue tests, the behavior of the material during a tensile test is used as a reference. Thereafter, σ_R and ε_R will respectively represent ultimate tensile strength and strain at failure. For both types of loading, stress at failure is lower than σ_R , nevertheless it is twice as high for static loading than for cyclic loading which means that cyclic loading has an effect on the material lifetime. Considering the strain at failure, the value is also lower for a cyclic loading than for a static loading. In addition, the elastic modulus decreases greatly before ultimate fracture of the composite while it tends to an asymptotic value for a static loading and does not reach the limit value $E_f \nu_f$. Moreover, the mean distance between matrix cracks in the longitudinal yarns is higher under cyclic fatigue, showing to saturation of matrix cracks could occur at a lower interfacial shear stress, decreased probably by progressive wear induced by cyclic loading. Under cyclic fatigue (Tab. 1), a greater proportion of recorded signals and a more significant release of energy were obtained at a given time than under static fatigue for the same values of temperature and maximum load. Thus this remark may point out an increase of damage due to loading cycles.

The figures 2a and 2b represent the evolution of the sentry function (F) during static and cyclic loading. In both cases, a third part appears for an average time of 90% of the total test duration. The function is then decreasing. The signals which have created this decrease are probably generated by fibers breakages since they are localized in the area where the specimen failed. The evolution of the sentry function during the cyclic fatigue test shows a part (part I.b) where the function is decreasing significantly. This is caused by the important increase of acoustic energy, whereas the strain remains constant. It appears that cyclic loading generates different types of damage since the

function does not show this type of variation for a static loading or a tensile test. The variations of this function in different cases exhibit different levels of damage on the composite: matrix cracking and fibers breakages for fatigue tests. Furthermore it shows that a cyclic loading has more critical damage effect than a static loading when the maximum stress is higher than 36 % of σ_R . In addition, during incremental fatigue test, this indicator reveals the fatigue limit (Fig. 2).

Now a focus is done on results obtained for cyclic loading at constant amplitude just behind this critical value. The evolution of R_{AE} coefficient versus time is given in Fig. 3. For the cyclic fatigue tests at constant amplitude, the evolution of the coefficient R_{AE} is very different from that observed in static fatigue. In both cases for the static fatigue, R_{AE} decreases first, down to a minimum value, and then increases up to the failure of the composite. On average, the minimum of R_{AE} appeared at 55% of the rupture time. The minimum of the coefficient R_{AE} indicates the beginning of the critical damage phase and provides an estimate of the remaining lifetime. In previous studies, the restart of activity prior to final rupture is attributed to the avalanche fibers ruptures. For the cyclic fatigue, a minimum value is not observed but a significant change of slope is visible for all mechanical tests at approximately 20-25% of the total test duration. This characteristic time could certainly be used in order to evaluate time to failure.

Table 1. Results of static and cyclic incremental fatigue tests

	Static fatigue (x2)	Cyclic fatigue (x3)
Stress at failure	84 % of σ_R	36-42 % of σ_R
Strain at failure	ϵ_R	0.36 % of ϵ_R
Elastic modulus at failure	$E_f v_f$	1.5 $E_f v_f$
Number of AE sources	9500	$2.57 \cdot 10^6$
Cumulated acoustic energy	$2.2 \cdot 10^8$ (attoJ)	$6.4 \cdot 10^{10}$ (attoJ)
matrix cracks spacing / matrix cracks spacing after tensile test	1	1.6

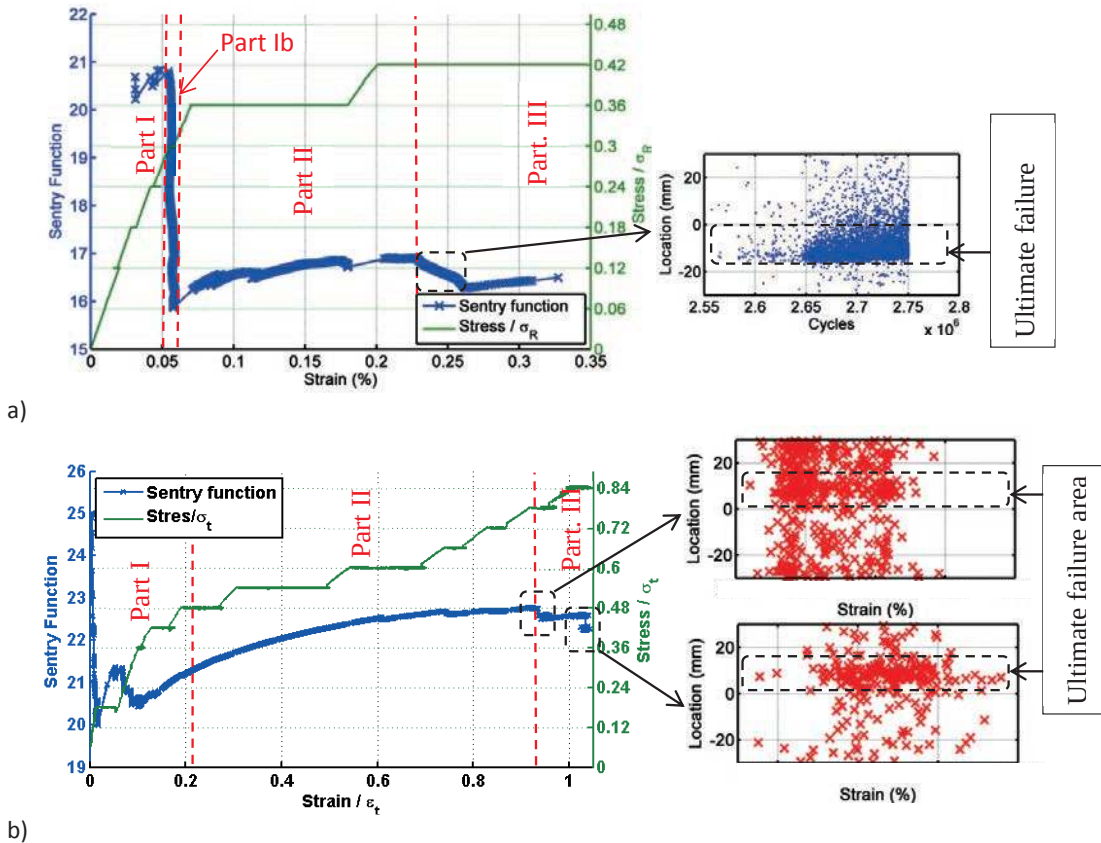


Figure 2 : Coupling of mechanical energy and acoustic energy (Sentry function) for a) an incremental cyclic fatigue test and b) an incremental static fatigue test

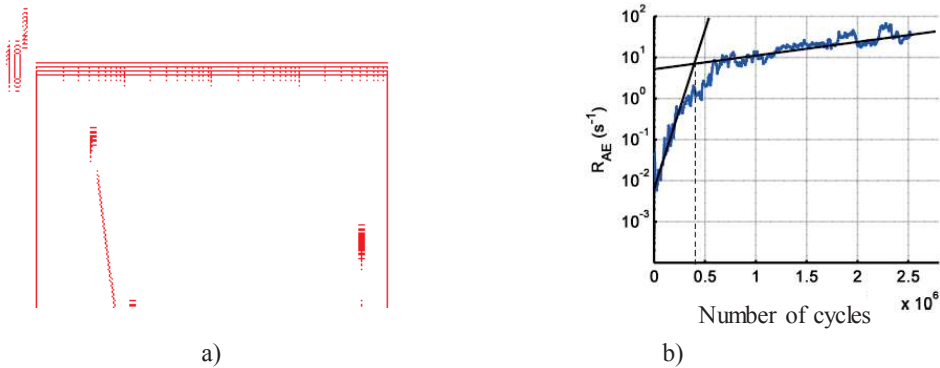


Figure 3 : Evolution of the coefficient R_{AE} a) for static fatigue test at constant stress with time b) for cyclic fatigue tests at constant amplitude with the number of cycles

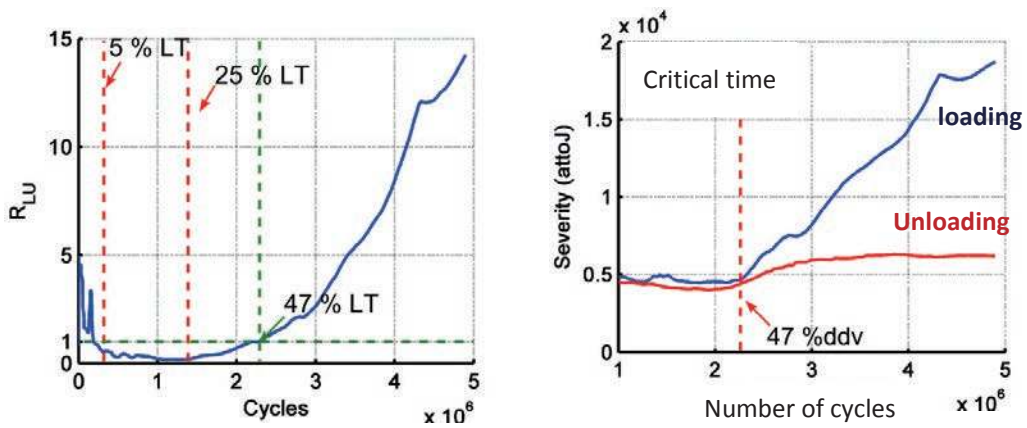


Figure 4: a) Evolution of the coefficient R_{LU} during cyclic fatigue at constant amplitude and highlight of two characteristic times at 25 % and 47 % of the lifetime duration (LT lifetime) on $SiC_f/[Si-B-C]$ composites, b) Evolution of the severity

Moreover, it is interesting to notice that the coefficient R_{LU} highlights two characteristic times before 50% of rupture time (Fig. 4a), the coefficient R_{LU} is again upper to 1 after the last characteristic time. After this characteristic time, the increase of the coefficient R_{LU} is linked to a significant increase of the severity of the signals recorded during the loading part (Fig. 4b). While for the signals recorded during the unloading phases, the severity remains constant. Moreover, the coefficient R_{LU} goes through a minimum around 25 % of rupture time.

A supervised classification technique can also be used to analyze AE signals recorded during fatigue of CMC composites in order to establish a link with the damage mechanism. This technique requires a data base of signals that have been labelled: the training set. This training set was created by merging data collected during tensile test. As described in the previous study, the analysis of AE signals, observation of microstructures and analysis of the mechanical behaviour of the composite led to the identification of 4 types of AE signals and to the following labelling of classes:

Class A: cluster A contains signals from two damage mechanisms which are chronologically well separated: seal coat cracking and tow breaks,

Class B: cluster B contains also signals from two damage mechanisms which are chronologically well separated: longitudinal matrix cracking and individual fibre breaks in the fracture zone just before failure,

Class C: Cluster C contains signals with relatively short duration, short rise time and low amplitude when compared to the others: transversal matrix cracking,

Class D: this cluster is the last one to be activated and it becomes more active as strain increases and the D-type signals have a longer rise time when compared to other signals: sliding at fibre/matrix interfaces, fibre/matrix debonding.

An additional class denoted E was introduced into the library. It corresponds to signals recorded under fatigue, during unloading steps of cycles after the cycle 2000e and for applied stresses lower than $\sigma_{max}/2 - 10$ MPa. These signals are associated to the friction generated in cyclic fatigue.

In order to establish the training set of labelled signals for the supervised analysis, the same amount of signals (2000 signals) in each class (A, B, C, D and E) was used. The cluster analysis with RFCAM algorithm pointed out different damage mechanisms generated by cyclic loading, which are mainly debonding and friction at matrix/fiber and matrix/matrix interfaces. Moreover, with this analysis a link is established between the characteristic time at 25 % and the beginning of the matrix cracking.

4 CONCLUSIONS

Comparison between static and cyclic tests shows that cyclic loading with an amplitude higher than 36 % of σ_R has significant effects on damage and on material lifetimes. Some new damage indicators are defined based on AE energy activity and dissipated mechanical energy. These new indicators show the evolution of damage during long term tests and can be used to propose new predictive laws of lifetimes. A link is established between a characteristic time at 25 % and the beginning of the matrix cracking for the cyclic fatigue tests.

ACKNOWLEDGEMENTS

The collaboration with Snecma and Herakles is gratefully acknowledged. This work was supported under the PRC Composites, French research project funded by DGAC, involving SAFRAN Group, ONERA and CNRS.

REFERENCES

- [1] J. Lamon (2005), CVI SiC/SiC composites NP. Bansal (Ed.), Handbook of ceramics composites, Springer.
- [2] O. Loseille, J. Lamon, (2010) Prediction of lifetime in static fatigue at high temperatures for ceramic matrix composites, *J. Adv. Mat. Res.*, 112:129-40.
- [3] GN. Morscher, (1999) Modal acoustic emission of damage accumulation in a woven SiC/SiC composite. *Compos Sci Technol*, 59, 687–697.
- [4] GN. Morscher, AL. Gyekenyesi (2002), The velocity and attenuation of acoustic emission waves in SiC/SiC composites loaded in tension. *Compos Sci Technol*, 62 pp 1171–1180.
- [5] M. Moevus, N. Godin, M. R'Mili, D. Rouby, P. Reynaud, G. Fantozzi and G. Farizy (2008), Analysis of damage mechanisms and associated acoustic emission in two SiCf/[Si-BC] composites exhibiting different tensile behaviours. Part II: Unsupervised acoustic emission data clustering, *Compos Sci Technol*, 68(6): 1258-1265.
- [6] S. Momon, N. Godin, P. Reynaud, M. R'Mili, and G. Fantozzi (2012), Unsupervised and supervised classification of AE data collected during fatigue test on CMC at high temperature, *Composites Part A*, 43(2): 254-260.
- [7] E. Maillet, N. Godin, M. R'Mili, P. Reynaud, G. Fantozzi, J. Lamon (2014), Damage monitoring and identification in SiC/SiC minicomposites using combined acousto-ultrasonics and acoustic emission, *Composites Part A*, 57 (8):15.
- [8] S. Momon, M. Moevus, M. R'Mili, P. Reynaud, G. Fantozzi and G. Fayolle (2010), Acoustic emission and lifetime prediction during static fatigue tests on ceramic-matrix-composite at high temperature under air, *Composites Part A*, 41(7): 913-918.
- [9] E. Maillet, N. Godin, M. R'Mili, P. Reynaud, G. Fantozzi and J. Lamon (2014), Real-time evaluation of energy attenuation: A novel approach to acoustic emission analysis for damage monitoring of ceramic matrix composites. *Journal of European Ceramic Society*, Volume: 34 Issue: 7, 1673-1679.
- [10] E. Maillet, N. Godin, M. R'Mili, P. Reynaud, J. Lamon and G. Fantozzi (2012), Analysis of Acoustic Emission energy release during static fatigue tests at intermediate temperatures on Ceramic Matrix Composites: Towards rupture time prediction, *Compos Sci Technol*, 72, 1001–1007.
- [11] N. Morizet, N. Godin, J. Tang, E. Maillet, M. Fregonese, B. Normand (2016), Classification of acoustic emission signals using wavelets and Random Forests : Application to localized corrosion. *Mechanical Systems and Signal Processing*, Volumes 70–71, 1026-1037.
- [12] G. Minak, P. Morelli, And A. Zucchelli (2009), Fatigue residual strength of circular laminate graphite–epoxy composite plates damaged by transverse load, *Compos Sci Technol*, vol. 69, no 9, 1358-1363.

- [13] G. Minak, And A. Zucchelli (2008), Damage evaluation and residual strength prediction of CFRP laminates by means of acoustic emission techniques, *Composite Materials Research Progress*. Nova Science Publishers, New York, 167-209.